Title: Altered immunity of laboratory mice in the natural environment is associated with fungal colonization

Authors: Frank Yeung[1,2,*], Ying-Han Chen[1,*], Jian-Da Lin[3,*], Jacqueline M. Leung[4], Caroline McCauley[3], Joseph C. Devlin[2,3], Christina Hansen[4], Alex Cronkite[1,3], Zac Stephens[5], Charlotte Drake-Dunn[1], Kelly V. Ruggles[6,7], June L. Round[5], P'ng Loke[3,§, †], Andrea L. Graham[4,§ ,†], and Ken Cadwell[1,3,§,†]

Affiliations:

[1]Kimmel Center for Biology and Medicine at the Skirball Institute,

[2]Sackler Institute of Graduate Biomedical Sciences,

[3]Department of Microbiology, New York University School of Medicine, New York, NY 10016, USA.

[4]Department of Ecology and Evolutionary Biology, Princeton University, Princeton, NJ 08544, USA.

[5]Division of Microbiology and Immunology, Department of Pathology, University of Utah School of Medicine, Salt Lake City, UT 84112, USA.

[6]Division of Translational Medicine, Department of Medicine,

[7]Applied Bioinformatics Laboratories, New York School of Medicine, New York, NY 10016, USA

*These authors contributed equally

†These authors contributed equally

[§]Correspondence to:

Ken.Cadwell@med.nyu.edu

Png.Loke@nyumc.org

algraham@princeton.edu

Abstract

The immune systems of free-living mammals such as humans and wild mice display a heightened degree of activation compared with laboratory mice maintained under artificial conditions. Here, we demonstrate that releasing inbred laboratory mice into an outdoor enclosure to mimic life in a natural environment alters the state of immunity. In addition to enhancing the differentiation of T cell populations previously associated with pathogen exposure, we found that outdoor release of mice led to an increase in circulating granulocytes. However, rewilded mice were not infected by pathogens previously implicated in immune activation. Rather, changes to the immune system were associated with an altered composition of the microbiota, and fungi isolated from rewilded mice were sufficient to increase granulocytes. These findings establish an experimental procedure to investigate the impact of the natural environment on immune development and identify a role for sustained fungal colonization in determining granulocyte numbers.

One sentence summary

Controlled release of laboratory mice into a natural environment changes the composition of the bacterial and fungal microbiota leading to an altered immune system.

Main text

Inbred laboratory mice are a staple of immunology research, yet fail to recreate certain aspects of human immunity. Recent findings suggest that this shortcoming of the rodent model may be due to the specific pathogen free (SPF) environment in which they are maintained. Wild mice and pet store mice, both of which are exposed to a litany of pathogens that are typically excluded from SPF facilities, display an abundance of differentiated memory T cells that more closely resembles the state of immunity in adult humans (*1-3*). Similarly, transferring embryos from lab mice into wild mice generates commensal- and pathogen-exposed offspring that more faithfully recreate human immunity than standard SPF mice, including the unresponsiveness to drugs that failed in clinical trials (*4*). Sequentially infecting SPF mice with 3 viruses and a helminth shifts the gene expression profile of peripheral blood mononuclear cells (PBMCs) towards that of pet store mice and adult humans (*5*), further highlighting the role for pathogen experience in normalizing the immune system. SPF mice are also distinguished from free-living mammals by the lack of exposure to potentially immuno-stimulatory members of the microbiota that are absent in a laboratory animal facility. For example, the offspring of germ-free mice inoculated with ileocecal contents from wild mice were shown to display increased resistance to influenza infection and colorectal tumorigenesis (*6*). However, the specific effect of the naturally-acquired microbiota on immune development is unclear, and the non-bacterial members of the wild microbiota such as fungi have not been examined in detail.

We recently described a mesocosm system in which SPF mice are 'rewilded' through controlled release into an outdoor enclosure facility (*7*). A key feature of the enclosure is that a zinced iron wall excludes predators and rodents harboring disease-causing infectious agents, while allowing exposure to natural soil, vegetation, and weather. Mice rewilded through transient release into the enclosure acquire a bacterial microbiota characterized by increased diversity, and display heightened susceptibility to helminth infection (*7*). To determine the consequence of microbial colonization in the natural environment on the steady-state immune system, we applied multicolor flow cytometry to analyze the immune cell composition of blood and mesenteric lymph nodes (MLNs) from SPF mice aged 6-8 weeks old at the time of release into the enclosure and captured 6-7 weeks later, herein referred to as rewilded mice. Details of the cohort of mice are described in Methods and includes male and female wild-type C57BL6/J mice, and also an additional cohort of mice harboring mutations in inflammatory bowel disease (IBD) genes

(*Atg16L1* and *Nod2*) that are the focus of the companion study (Lin *et. al.*). Matched control mice were maintained under SPF conditions in the institutional vivarium, herein referred to as lab mice. Similar to wild or pet store mice (*1, 2, 4, 6*), we observed an increase in differentiated $CD8^+$ and $CD4^+$ T cells with surface markers identifying them as $CD62L^{lo}CD44^{hi}$ effector memory (T_{EM}) and $CD62L^{hi}CD44^{hi}$ central memory (T_{CM}) populations, and a corresponding decrease in $CD62L^{hi}CD44^{lo}$ naïve T cells in rewilded mice compared with lab mice (Fig. 1A and fig. S1, A to C). We also observed an increase in $CD8^+$ and $CD4^+$ T cells expressing activation markers KLRG1 and CD25, respectively (Fig. 1B and C, and fig. S2A). Histological examination of the small intestine and colonic tissue from rewilded mice revealed an increased number of $CD8^+$ cells (Fig. 1D). Despite these features of enhanced immune activation, we did not detect histopathology in intestinal sections (fig. S1D). Thus, rewilding is associated with a general enhancement in T cell maturation resembling observations made in pet store mice.

In addition to these expected changes to the lymphocyte compartment, we found a striking increase in the side scatter high (SSC^{hi}) fraction of PBMCs and cells harboring myeloid markers in rewilded mice compared with lab mice, indicating that release into the outdoor enclosure induced an enrichment in granulocytes (Fig. 1E). Similarly, we observed an increase in neutrophils in the MLNs of rewilded mice (Fig. 1F and fig. S2B). RNA-Seq analysis comparing MLNs from lab and rewilded mice indicated that release into an outdoor enclosure increases the expression of genes involved in T cell differentiation and leukocyte migration (Fig. 1G). These immune profiling experiments indicate that rewilding leads to an immune system with hallmarks of increased activation and differentiation of multiple cell types.

Furthermore, and in stark contrast to pet store mice (*1*), rewilded mice were negative for all of the pathogens tested in a comprehensive serology panel (fig. S3). We also failed to detect the presence of pathogens using an extended PCR-based analysis, albeit a subset of mice was positive for opportunistic pathogens that are frequently found in SPF facilities, such as *Proteus mirabilis* (fig. S4). Therefore, we turned our attention to the microbiota as a potential source of immune activation. 16S rDNA sequencing of stool samples indicated that rewilding was associated with enrichment of *Bacteroides* and related taxa, and a decrease in Firmicutes such as *Lactobacillus* and *Faecalibaculum* species (Fig. 2, A to C). However, these changes were modest compared with the large increase in *Bacteroides* reported in a prior study examining the microbiota of wild mice (*6*), likely reflecting the fact that in our system, adult mice are released

into the wild environment with an intact microbiota. Intestinal colonization by commensal fungi (mycobiota) can also contribute to immunity (*8-16*). Quantification of fungal burden by qPCR of the conserved ITS region on the same samples above indicated that rewilded mice harbor a significant increase in intestinal colonization by fungi compared with lab mice (Fig. 2D).

The changes to the bacterial and fungal microbiota led us to ask whether cytokine responses to different microbial stimuli are altered after exposure to a natural environment. Single cell suspensions of MLNs from rewilded and lab mice were incubated with a panel of UV-killed microbes, PBS as a negative control, and αCD3/CD28 beads as a positive control that non-specifically activates T cells. In contrast to the unstimulated PBS control condition, MLN cells derived from rewilded mice responded to microbial or T cell stimulation by secreting generally higher amounts of cytokines and chemokines compared to cells derived from lab mice (Fig. 2E; over and above differences among genotypes described by companion study, Lin *et. al.*). The exact cytokines that were over-produced were specific to the microbial stimulant, although some general trends include 2–10-fold increases in IL-17, CXCL1, CCL3, and IL-10. Consistent with the increased fungal colonization that occurs in the natural environment, stimulation *in vitro* with the model fungus *Candida albicans*, which frequently colonizes the gastrointestinal tract of humans, led to a particularly striking difference between cells from rewilded versus lab mice. These results suggest that immune cells of rewilded mice are in a hyperactivated state due to exposure to natural microbes, including fungi.

The effects of rewilding could be a response to a number of possible environmental variables, including diversification of diet and activity levels outdoors (e.g., (*19*)). To determine whether the enhanced activation and maturation of the immune system was due to changes in microbial exposure, germ-free mice were reconstituted with microbiota through inoculation with cecal contents from rewilded mice and lab mice, and then blood and MLNs harvested from their offspring were analyzed by flow cytometry. Mice harboring the microbiota of rewilded mice displayed an increase in granulocytes including neutrophils (Fig. 3, A and B). However, this increase was modest compared with the rewilded mice that served as donors. 16S rDNA sequencing showed that the bacterial community structures were preserved in the offspring of the germ-free mice reconstituted with cecal contents (fig. S5). In contrast, quantification of total fungal burden indicated that fungal colonization was reduced in the progeny of reconstituted mice (Fig. 3C). These results raise the possibility that sustained exposure to a high fungal burden

is necessary to recreate the full effect of rewilding. To test this possibility, we inoculated antibiotics-treated conventional mice with *C. albicans* as a model of high fungal colonization. Intestinal colonization by *C. albicans* occurs in the majority of adult humans and is associated with enhanced Th17 $CD4^+$ T cell differentiation (*20*, *21*). Mice colonized by *C. albicans* displayed a substantial increase in granulocytes and neutrophils (Fig. 3D). These immune cell composition changes were not due to systemic infection as *C. albicans* colonization was restricted to the gut in this model (Fig. 3E). Inoculation of germ-free mice with *C. albicans* also reproduced the increase in granulocytes demonstrating that fungal colonization is sufficient, though this approach led to a lower amount of *C. albicans* colonization, and a corresponding less dramatic change in granulocyte numbers (Fig. 3F and fig. S6A). To further demonstrate that fungal burden directly influences granulocyte numbers, we treated *C. albicans* mono-associated mice with the antifungal drug flucozanole. Our results show that decreasing fungal burden leads to a further decrease in granulocytes, indicating that the degree of intestinal colonization by fungi impacts the proportion of immune cells in the periphery (Fig. 3F and fig. S6B).

Having determined that exposure to the natural environment leads to an increase in fungal burden, we next used ITS sequencing of stool to compare the composition of the fungal microbiota of rewilded and lab mice. We found that rewilding led to major changes, most notably an enrichment in *Aspergillus* species (Fig. 4, A to D). We were able to isolate many of the fungi corresponding to the taxa identified in the sequencing reads when we plated stool from rewilded mice on Sabouraud dextrose agar (Fig. 4E), but were unable to grow any fungi from lab mice. Finally, we gavaged conventional mice and germ-free mice with a consortium of representative "wild" fungi consisting of *Aspergillus candidus*, *Aspergillus proliferans*, *Chaetomium globosum* and *Dichotomopilus Indicus* (corresponding to plates (i)–(vii) depicted in Fig. 4E) and found that they were able to induce the increase in peripheral granulocytes and neutrophils (Fig. 4, F and G). Thus, exposure to fungi in the natural environment can contribute to the state of the immune system.

In conclusion, we found that releasing laboratory mice into a natural environment, even for a limited amount of time, can reproduce the enhanced differentiation of memory T cells previously attributed to infection by life-threatening pathogens. Additionally, we identified granulocyte expansion as a key feature of exposure to the natural environment, which was associated with fungal microbiota. These findings are notable because granulocytes are abundant

in human blood and scarce in laboratory mice. We suggest that this difference in blood immune cell populations between species is due to environmental variables. Altogether, the findings presented here expand our understanding of the immunomodulatory role of intestinal fungi and indicate that a diverse fungal microbiota, likely together with the bacterial microbiota, participates in the differentiation of the immune system in a free-living mammal.

References

1. L. K. Beura *et al.*, *Nature* **532**, 512 (Apr 28, 2016).
2. S. Abolins *et al.*, *Nature communications* **8**, 14811 (May 3, 2017).
3. Y. J. Choi *et al.*, *Nat Immunol* **20**, 276 (Mar, 2019).
4. S. P. Rosshart *et al.*, *Science* **365**, (Aug 2, 2019).
5. T. A. Reese *et al.*, *Cell Host Microbe* **19**, 713 (May 11, 2016).
6. S. P. Rosshart *et al.*, *Cell* **171**, 1015 (Nov 16, 2017).
7. J. M. Leung *et al.*, *PLoS Biol* **16**, e2004108 (Mar, 2018).
8. I. D. Iliev *et al.*, *Science* **336**, 1314 (Jun 8, 2012).
9. M. L. Wheeler *et al.*, *Cell Host Microbe* **19**, 865 (Jun 8, 2016).
10. I. Leonardi *et al.*, *Science* **359**, 232 (Jan 12, 2018).
11. X. Li *et al.*, *Cell Host Microbe* **24**, 847 (Dec 12, 2018).
12. J. J. Limon *et al.*, *Cell Host Microbe* **25**, 377 (Mar 13, 2019).
13. T. T. Jiang *et al.*, *Cell Host Microbe* **22**, 809 (Dec 13, 2017).
14. T. R. Chiaro *et al.*, *Sci Transl Med* **9**, (Mar 8, 2017).
15. G. H. W. Tso *et al.*, *Science* **362**, 589 (Nov 2, 2018).
16. Z. Zhang *et al.*, *Immunity* **44**, 330 (Feb 16, 2016).
17. J. Martinez *et al.*, *Nat Cell Biol* **17**, 893 (Jul, 2015).
18. T. Akoumianaki *et al.*, *Cell Host Microbe* **19**, 79 (Jan 13, 2016).
19. S. A. Budischak *et al.*, *Front Immunol* **8**, 1914 (2018).
20. P. Bacher *et al.*, *Cell* **176**, 1340 (Mar 7, 2019).
21. T. Y. Shao *et al.*, *Cell Host Microbe* **25**, 404 (Mar 13, 2019).

Acknowledgements

We wish to thank William Craigens, Daniel Navarrete Prado, Allison Lee, and Veena Chittamuri for assistance with trapping and husbandry in the field, the PU Lab Animal Resources staff for logistical support. We wish to thank the NYU School of Medicine Flow Cytometry and Cell Sorting, Microscopy, Genome Technology, and Histology Cores for use of their instruments and technical assistance (supported in part by National Institute of Health (NIH) grant P31CA016087, S10OD01058, and and S10OD018338). We also wish to thank Margie Alva, Juan Carrasquillo,

and Beatriz Delgado for technical assistance with gnotobiotics. **Funding:** this research was supported by US National Institute of Health (NIH) grants DK103788 (K.C. and P.L.), AI121244 (K.C.), HL123340 (K.C.), DK093668 (K.C.), AI130945 (P.L.), R01 HL125816 (K.C.), HL084312, AI133977 (P.L.), research station and research rebate awards from PU EEB (A.L.G.), pilot award from the NYU CTSA grant UL1TR001445 from the National Center for Advancing Translational Sciences (NCATS) (K.C., P.L.), pilot award from the NYU Cancer Center grant P30CA016087 (K.C.), AI100853 (Y.C.), and DK122698 (F.Y.). This work was also supported by the Department of Defense grant W81XWH-16-1-0256 (P.L.), Faculty Scholar grant from the Howard Hughes Medical Institute (K.C.), Crohn's & Colitis Foundation (K.C.), Merieux Institute (K.C.), Kenneth Rainin Foundation (K.C.), Stony-Wold Herbert Fund (K.C.), and Bernard Levine Postdoctoral Research Fellowship in Immunology (Y.C.). K.C. is a Burroughs Wellcome Fund Investigator in the Pathogenesis of Infectious Diseases. **Author contributions:** Design of experiments, data analysis, data discussion, and interpretation: F.Y., Y.H.C., J.D.L., J.C.D., P.L., A.L.G., and K.C; primary responsibility for execution of experiments: F.Y., Y.H.C., J.D.L., J.M.L., C.M., A.C., Z.S., and C.D.D.; MLN cell RNA, 16S and ITS sequencing analysis: J.C.D., J.L.R., K.V.R., Z.S., F.Y., and Y.H.C. All authors discussed data and commented on the manuscript. **Competing interests:** K.C. and P.L. receive research funding from Pfizer. K.C. has consulted for or received an honorarium from Puretech Health, Genentech, and Abbvie. P.L. consults for and has equity in Toilabs. **Data and materials availability:** Raw sequence data from 16*S* , ITS, and RNA sequencing experiments are deposited in the NCBI Sequence Read Archive under BioProject accession number PRJNA559026 and gene expression omnibus (GEO) accession number GSE135472.

Figure Legend:

Figure 1. Rewilding alters the proportion of lymphoid and myeloid cell subsets.
(**A**) Representative flow cytometry plots and quantification of $CD62L^{hi}CD44^{lo}$ (naive), $CD62L^{hi}CD44^{hi}$ (central memory) and $CD62L^{lo}CD44^{hi}$ (effector memory) $CD8^{+}$ T cells in the peripheral blood of rewilded mice (Wild) and control mice maintained in the laboratory condition (Lab). Cells were gated on $Live^{+}CD45^{+}Myeloid^{-}CD3^{+}CD19^{-}CD8^{+}$. N = 79 lab and 101

rewilded mice (**B**) Mean fluorescent intensity of MLN $CD8^+$ T cells expressing activation marker KLRG1. (**C**) Quantification of the proportion of MLN cells expressing $CD4^+CD25^+$. N = 77 lab and 101 rewilded mice. (**D**) Representative images of small intestinal sections stained for $CD8^+$ cells and quantification. N = 50 villi from 3 mice per condition. (**E**) Representative forward scatter (FSC) and side scatter (SSC) flow cytometry plots and quantification of SSC^{hi} cells (granulocytes) and myeloid cells in the peripheral blood of lab and rewilded mice. All cells were gated on $Live^+CD45^+$ and myeloid cells were identified by cell surface markers CD11b/CD11c/DX5. N = 79 lab and 101 rewilded mice. (**F**) Quantification of the absolute number of MLN cells expressing neutrophil markers ($CD11b^+Ly6G^+$). (**G**) Functional classification of differentially regulated genes by Ingenuity pathway analysis comparing RNA-Seq of MLN cells from lab and rewilded mice. The arrowed line marks where the p-value becomes less than 0.05. N = 40 lab and 46 rewilded mice. **** $P < 0.0001$ by two-tailed Student's *t*-test between groups, (A) to (F).

Figure 2. Altered immunity in rewilded mice is associated with microbial exposure in the natural environment.

(**A**) Stacked bar plot of mean relative abundances of genus level taxa that constitute the fecal microbial community of lab (Lab) and rewilded (Wild) mice as determined by 16S sequencing. N = 79 lab and 102 rewilded mice. **(B)** Alpha diversity quantification through number of operational taxonomic units (OTUs) from (A). **(C)** Bacterial taxa from (A) significantly enriched in lab versus wild conditions as determined by discrete-false discovery rate (DS-FDR) analysis. (**D**) Quantification of relative fungal burden in stool of lab and rewilded mice as determined by qPCR of the internal transcribed space (ITS) region normalized to the average of lab mice. (**E**) Radar plots showing the amount of each indicated cytokine/chemokine produced by MLN cells after stimulation with αCD3/CD28 beads and the following microbes: *Bacillus subtilus*, *Bacteroides vulgatus*, *Candida albicans*, *Clostrdium perfringens*, and *Staphylococcus aureus*. Data represents Log2 fold change over MLN cells unstimulated PBS controls. ** P <0.01 by two-tailed Student's *t*-test between groups, (C).

Figure 3. Altering the microbiota of lab mice recreates expansion of granulocytes observed in rewilded mice.

(**A**) Representative flow cytometry plots and quantification of SSC^{hi} cells and myeloid cells (CD11b/CD11c/DX5) gated on $Live^{+}CD45^{+}$ in the peripheral blood of the F1 progeny from germ-free (GF) mice reconstituted with cecal contents from lab (Lab) and rewilded (Wild) mice. N>10 recipient mice per condition were reconstituted with 3 donor lab and rewilded mice each. Data represents 2 independent repeats. (**B**) Quantification of the proportion of neutrophils ($CD11b^{+}Ly6G^{+}$) in the peripheral blood from the mice in (A). (**C**) Quantification of the relative fungal burden in stool of mice from (A) as determined by ITS qPCR. N = 3 and 5 mice reconstituted with lab and GF cecal contents from (A), respectively. (**D**) Quantification of SSC^{hi} cells and neutrophils in the peripheral blood from antibiotic-treated conventional mice 4 weeks post-inoculation with PBS or *C. albicans*. N = 5 mice per group, 2 independent repeats. (**E**) Colony forming units (CFUs) of fungi in feces and indicated organs for mice from (D). Dotted line denotes limit of detection (L.O.D.). (**F**) Linear regression analysis comparing frequency of neutrophils in the blood and fungal CFUs in feces from antibiotics treated mice inoculated with *C. albicans*(ABX+CA) from (D), germ-free mice mono-associated with *C. albicans* (GF+CA), and germ-free mice mono-associated with *C. albicans* and treated with fluconazole (GF+CA+Fluconazole). N = 5 ABX+CA, 4 GF+CA, and 3 GF+CA+Fluconazole. * $P < 0.05$, ** $P < 0.01$, *** $P < 0.001$ by two-tailed Student's *t*-test between groups, (A) to (D).

Figure 4. Rewilding leads to colonization by immunomodulatory fungi.

(**A**) Beta diversity (Bray Curtis) plots of fungal taxa detected by ITS sequencing of stool from lab (Lab) mice (purple dots) and rewilded (Wild) mice (red dots). N = 24 lab and 25 rewilded mice. (**B**) Alpha diversity quantification through number of operational taxonomic units (OTUs) from (A). (**C**) Number of ITS sequencing reads corresponding to the indicated genus from (A). (**D**) Fungal species from (A) significantly enriched in lab versus wild conditions by DS-FDR analysis. (**E**) Representative images of colonies growing on Sabouraud dextrose agar plates following plating of cecal suspensions harvested from rewilded mice corresponding to (i) *Aspergillus proliferans*, (ii) *Aspergillus proliferans*, (iii) *Aspergillus proliferans*, (iv) *Aspergillus candidus*, (v) *Aspergillus sp.*, (vi) *Chaetomium globosum*, (vii) *Dichotomopilus indicus*, (viii) *Aspergillus niger*, (ix) *Malbranchea flavorosea*, (x) *Talaromyces tratensis*, (xi) *Syncephalastrum racemosum*, (xii) *Talaromyces tratensis*. (**F**) Frequency of SSC^{hi} cells and neutrophils in peripheral blood from conventional mice repetitively gavaged with a consortium of 7 wild fungi

isolates from plates (i)–(vii) in (E) or PBS for 2 weeks. N = 4 mice per group. **(G)** Frequency of SSC^{hi} cells and neutrophils in the peripheral blood from germ-free mice 2 weeks post-inoculation with a consortium of 7 wild fungi. N = 8 mice per group, 2 independent repeats. * P <0.05, **** *P* < 0.0001 by two-tailed Student's *t*-test between groups, (B), (F), and (G).

Supplemental Figure 1. Rewilding increases central memory and effector memory T cell populations.

Additional quantification of T cell subsets from rewilded (Wild) mice and control mice maintained in the laboratory condition (Lab) described in Figure 1. (**A**) Quantification of $CD62L^{hi}CD44^{lo}$ (naïve), $CD62L^{hi}CD44^{hi}$ (central memory) and $CD62L^{lo}CD44^{hi}$ (effector memory) $CD4^{+}$ T cells in the peripheral blood. (**B**) Quantification of naïve, central memory and effector memory $CD8^{+}$ T cells in the mesenteric lymph nodes (MLNs). (**C**) Quantification of naïve, central memory, and effector memory $CD4^{+}$ T cells in the MLNs. (**D**) Representative H&E stained small intestinal sections. N = 79 lab and 101 wild mice (Blood); N = 77 lab and 101 rewilded mice (MLN). **** *P* < 0.0001 by two-tailed Student's *t*-test between groups, (A) to (C).

Supplemental Figure 2. Flow cytometry analysis of lymphoid and myeloid cells expanded in the mesenteric lymph nodes of rewilded mice.

(**A**) Representative flow cytometry plots of mesenteric lymph node (MLN) cells expressing $CD4^{+}CD25^{+}$. (**B**) Representative flow cytometry plots of MLN cells expressing $CD11b^{+}Ly6G^{+}$. All cells were gated on $Live^{+}CD45^{+}CD19^{-}CD3^{-}$. Data corresponds to mice in Fig. 1 and quantification of these cell populations in the main figure.

Supplemental Figure 3. Rewilded mice are seronegative for common mouse pathogens.

Multiplexed Fluorometric ImmunoAssay results from serum of lab (Lab) and rewilded (Wild mice (Animal Health Diagnostic Services, MFIA Mouse Assessment Plus Profile, Charles River). N = 5 lab and 5 rewilded mice.

Supplemental Figure 4. PCR panel for mouse pathogens and commensals comparing rewilded and lab mice.

TaqMan PCR testing results from direct animal sampling of lab (Lab) and rewilded (Wild) mice (Animal Health Diagnostic Services, Surveillance Plus PRIA Panel, Charles River). N = 5 lab and 20 rewilded mice.

Supplemental Figure 5. Bacterial community structure of germ-free mice reconstituted with microbiota from lab and rewilded mice.

Stacked bar plot indicates the mean relative abundances of genus level taxa that make up the fecal microbial communities in lab (Lab), rewilded (Wild) mice, or germ-free (GF) mice reconstituted with cecal contents from either lab or rewilded mice. N>5 recipient mice per condition.

Supplemental Figure 6. *Candida albicans* mono-colonization increases neutrophils in the peripheral blood.

(**A**) Quantification of $CD11b^{+}Ly6G^{+}$ neutrophils in the peripheral blood of *C. albicans* (CA) mono-associated and control mice (PBS). (**B**) Quantification of neutrophils in the peripheral blood of *C. albicans* mono-associated mice after treatment with antifungal drug (Fluconazole) for 4 weeks. N = 4 mice per condition. * $P < 0.05$ by two-tailed Student's *t*-test between groups.

Figure 1

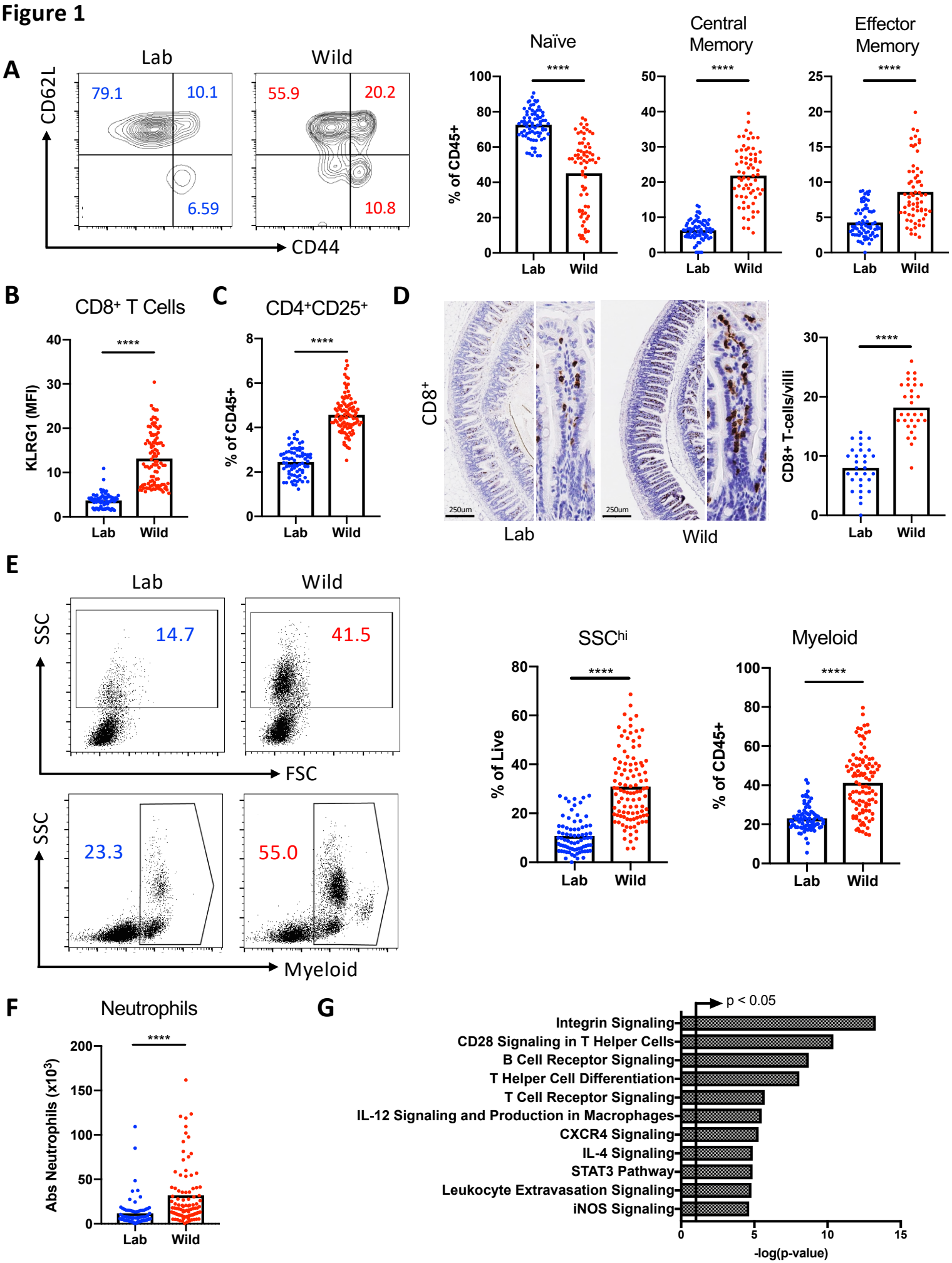
A
Lab
Wild
CD62L
CD44
79.1
10.1
6.59
55.9
20.2
10.8
Naïve
Central Memory
Effector Memory
% of CD45+
****
Lab
Wild
B
CD8+ T Cells
KLRG1 (MFI)
C
CD4+CD25+
% of CD45+
D
CD8+
250um
CD8+ T-cells/villi
E
SSC
FSC
14.7
41.5
23.3
55.0
Myeloid
SSChi
% of Live
F
Neutrophils
Abs Neutrophils (x10³)
G
p < 0.05
Integrin Signaling
CD28 Signaling in T Helper Cells
B Cell Receptor Signaling
T Helper Cell Differentiation
T Cell Receptor Signaling
IL-12 Signaling and Production in Macrophages
CXCR4 Signaling
IL-4 Signaling
STAT3 Pathway
Leukocyte Extravasation Signaling
iNOS Signaling
-log(p-value)

Figure 2

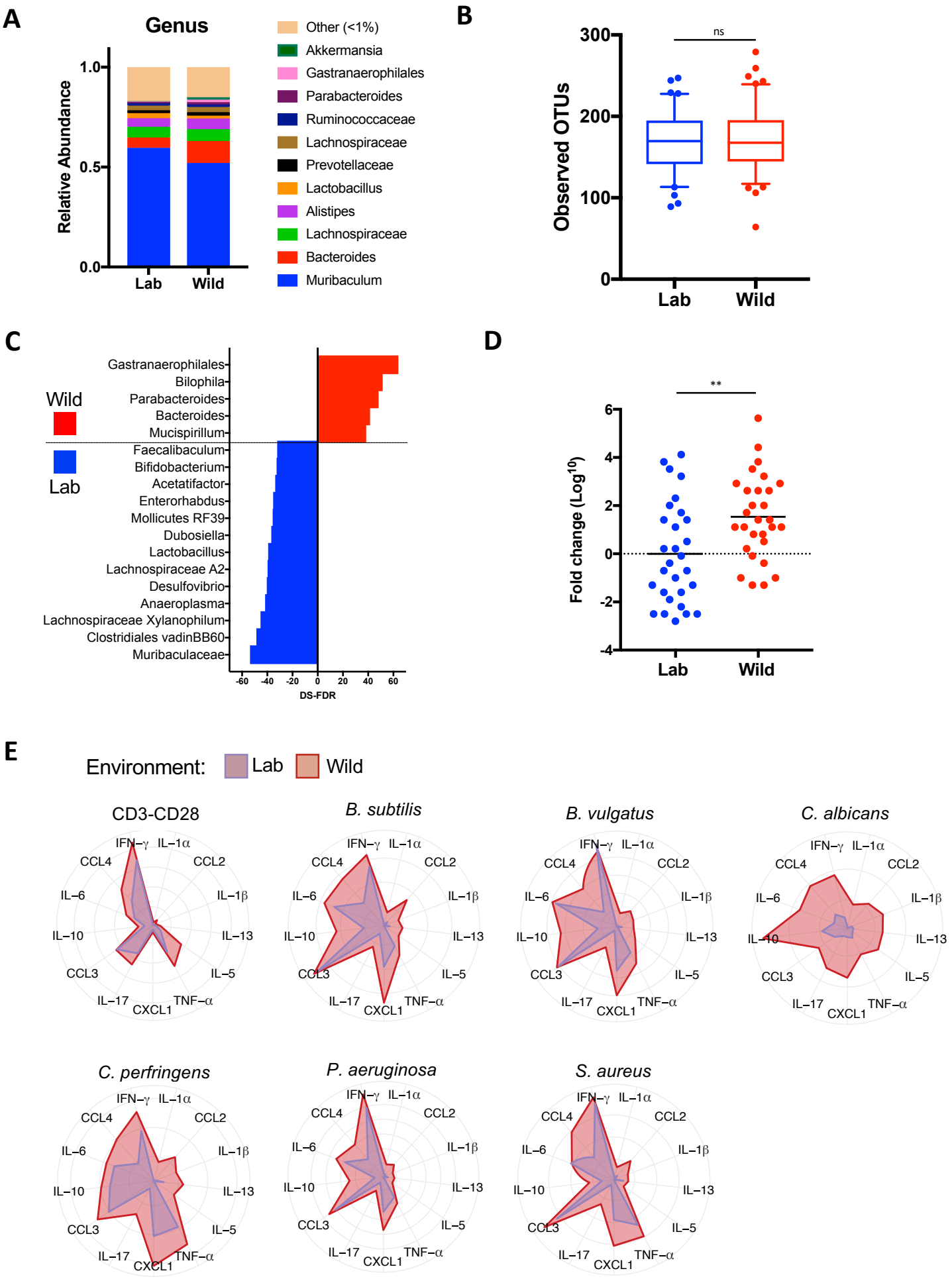
A
Genus
Relative Abundance
1.0
0.5
0.0
Lab
Wild
Other (<1%)
Akkermansia
Gastranaerophilales
Parabacteroides
Ruminococcaceae
Lachnospiraceae
Prevotellaceae
Lactobacillus
Alistipes
Lachnospiraceae
Bacteroides
Muribaculum
B
Observed OTUs
300
200
100
0
ns
Lab
Wild
C
Wild
Lab
Gastranaerophilales
Bilophila
Parabacteroides
Bacteroides
Mucispirillum
Faecalibaculum
Bifidobacterium
Acetatifactor
Enterorhabdus
Mollicutes RF39
Dubosiella
Lactobacillus
Lachnospiraceae A2
Desulfovibrio
Anaeroplasma
Lachnospiraceae Xylanophilum
Clostridiales vadinBB60
Muribaculaceae
-60 -40 -20 0 20 40 60
DS-FDR
D
Fold change (Log10)
6
4
2
0
-2
-4
**
Lab
Wild
E
Environment: Lab Wild
CD3-CD28
B. subtilis
B. vulgatus
C. albicans
C. perfringens
P. aeruginosa
S. aureus
IFN-γ
IL-1α
CCL2
IL-1β
IL-13
IL-5
TNF-α
CXCL1
IL-17
CCL3
IL-10
IL-6
CCL4

Figure 3

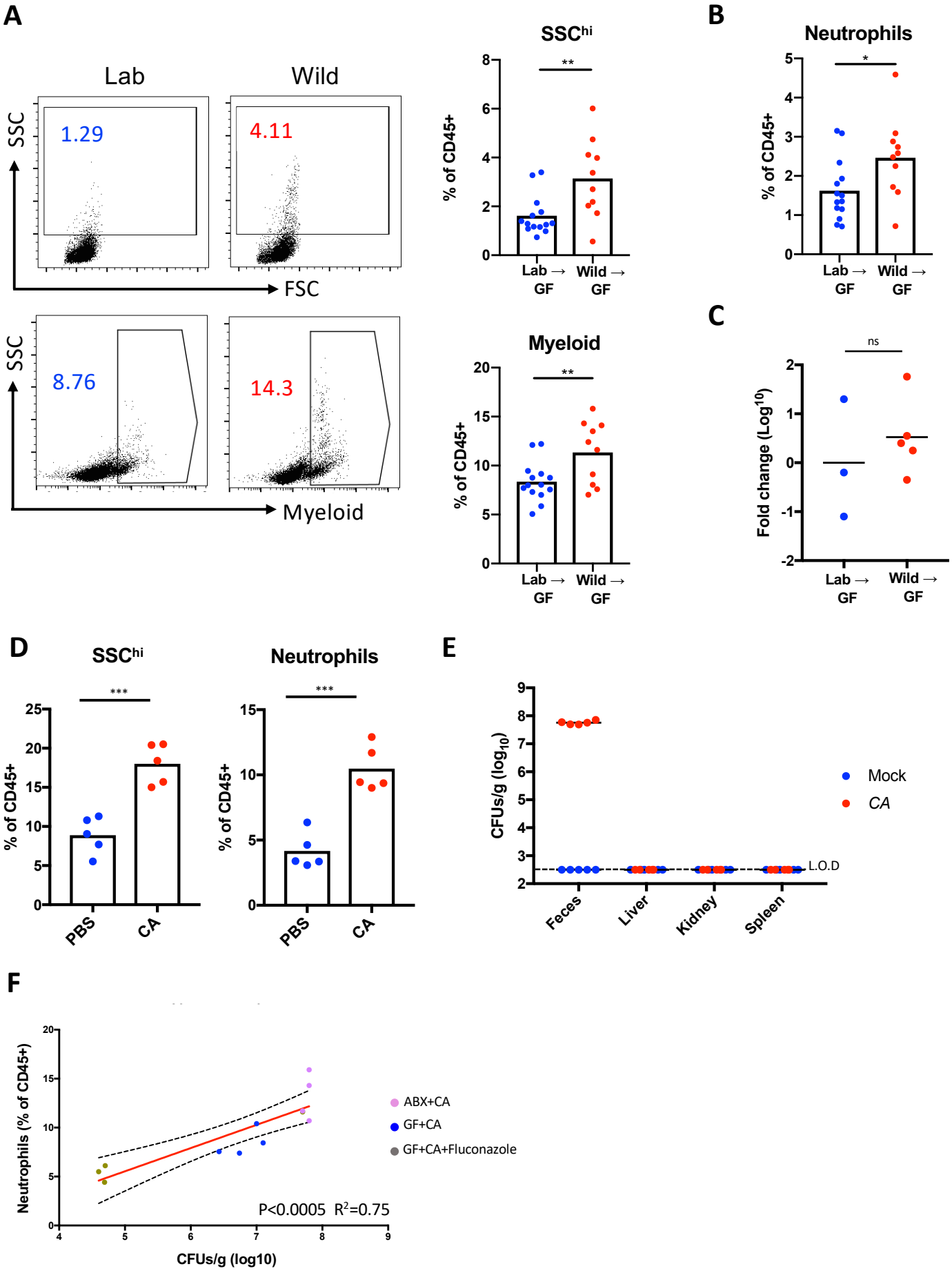
A
Lab
Wild
SSC
1.29
4.11
FSC
8.76
14.3
Myeloid
SSC^hi
% of CD45+
**
Lab → GF
Wild → GF
Myeloid
B
Neutrophils
*
C
ns
Fold change (Log10)
D
SSC^hi
Neutrophils
***
PBS
CA
E
CFUs/g (log10)
Mock
CA
L.O.D
Feces
Liver
Kidney
Spleen
F
Neutrophils (% of CD45+)
ABX+CA
GF+CA
GF+CA+Fluconazole
P<0.0005 R2=0.75
CFUs/g (log10)

Figure 4

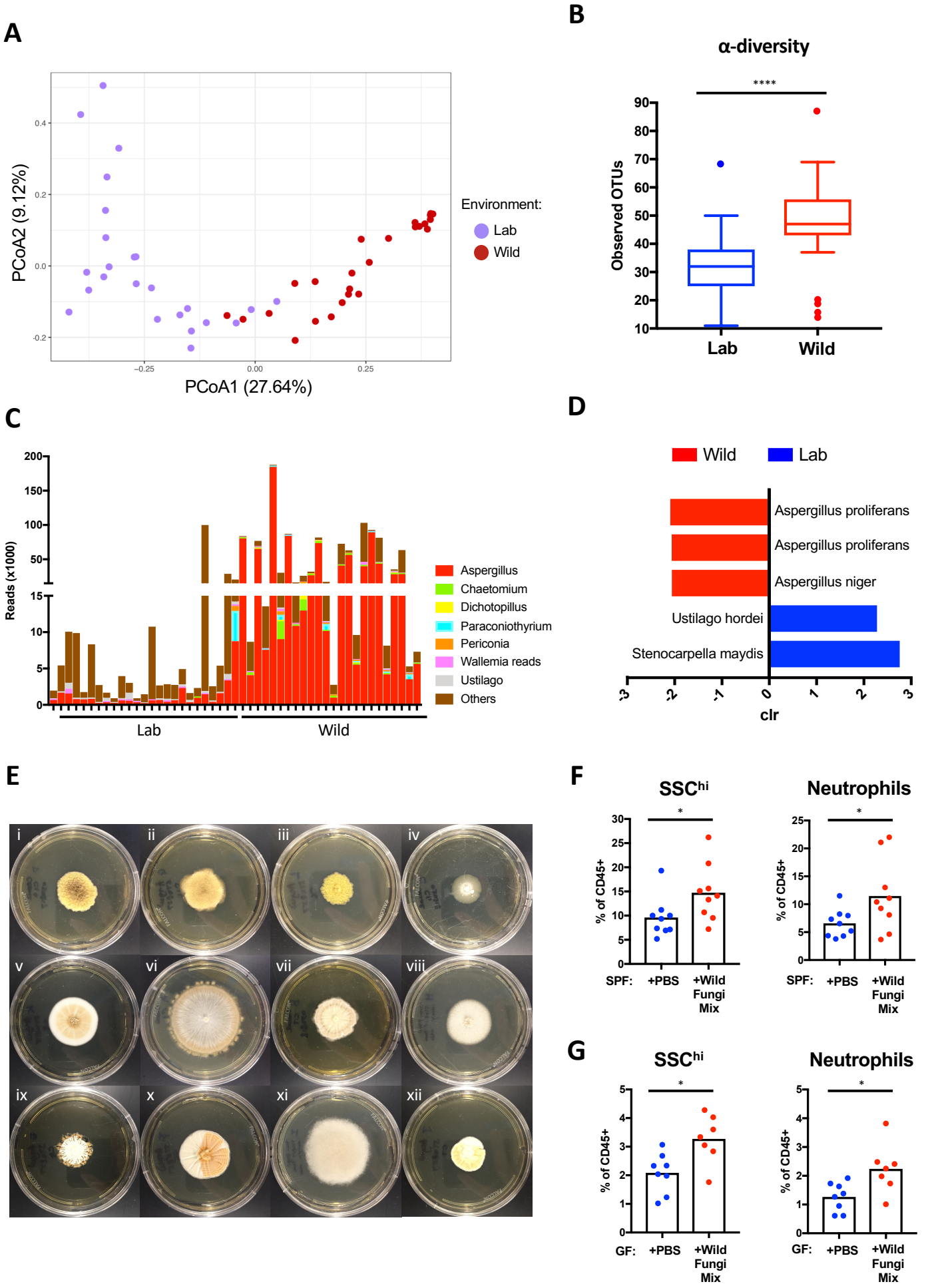
A
PCoA2 (9.12%)
PCoA1 (27.64%)
Environment:
Lab
Wild
B
α-diversity
****
Observed OTUs
Lab
Wild
C
Reads (x1000)
Aspergillus
Chaetomium
Dichotopillus
Paraconiothyrium
Periconia
Wallemia reads
Ustilago
Others
Lab
Wild
D
Wild
Lab
Aspergillus proliferans
Aspergillus proliferans
Aspergillus niger
Ustilago hordei
Stenocarpella maydis
clr
E
i
ii
iii
iv
v
vi
vii
viii
ix
x
xi
xii
F
SSChi
Neutrophils
% of CD45+
SPF:
+PBS
+Wild Fungi Mix
G
SSChi
Neutrophils
% of CD45+
GF:
+PBS
+Wild Fungi Mix

Supplemental 1

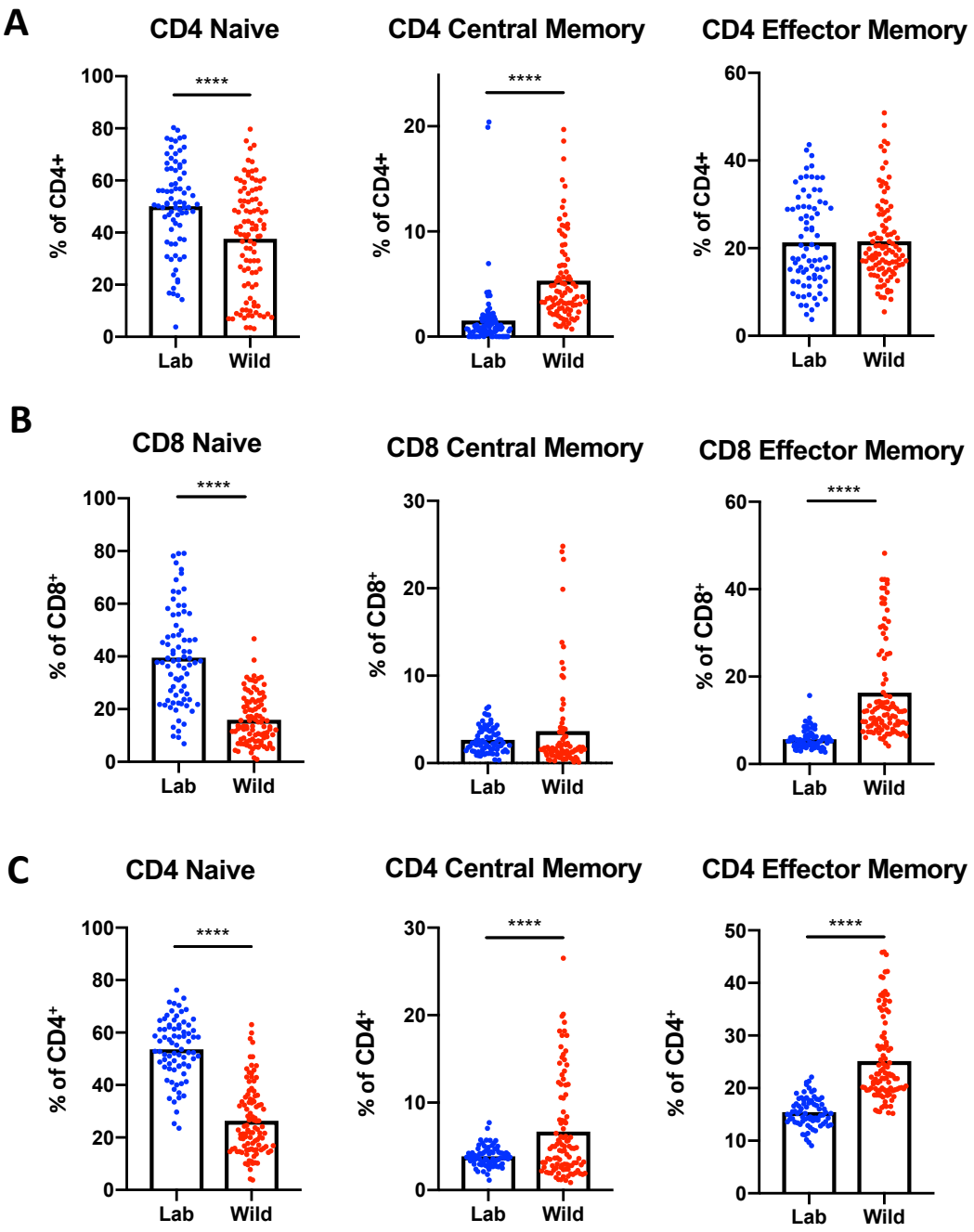

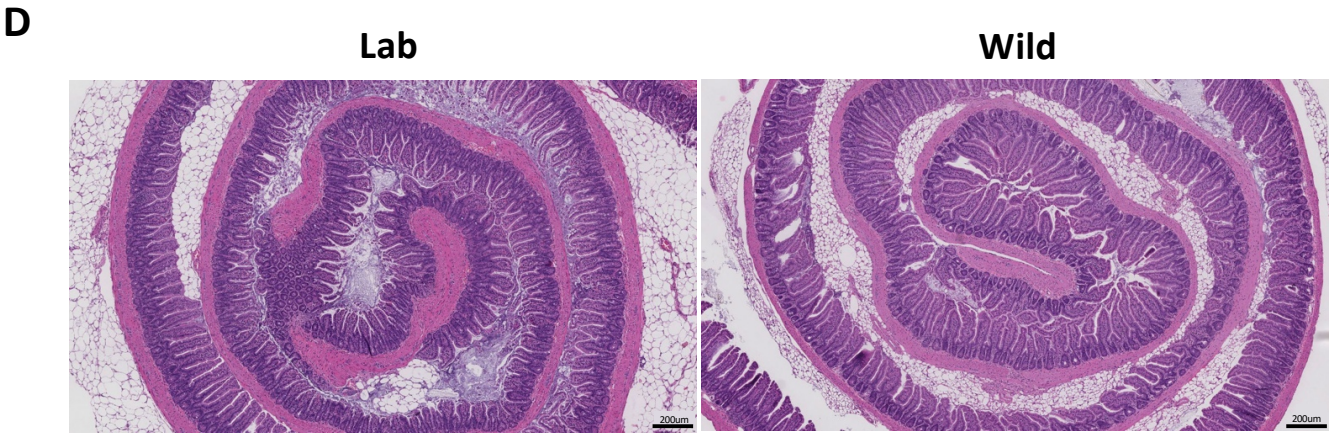

Supplemental 2

A

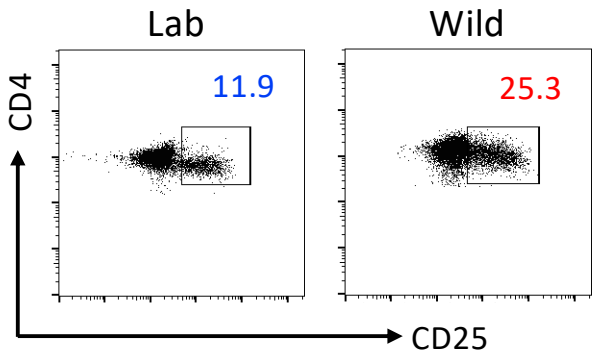

B

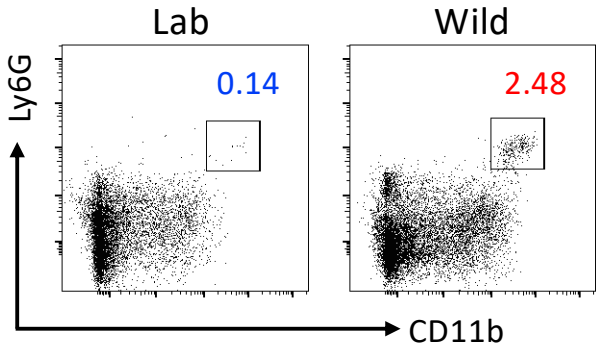

Supplemental 3

Serology	Lab	Wild
MFIA SEND	0/5 (0%)	0/5 (0%)
MFIA PVM	0/5 (0%)	0/5 (0%)
MFIA MHV	0/5 (0%)	0/5 (0%)
MFIA MVM	0/5 (0%)	0/5 (0%)
MFIA MPV1	0/5 (0%)	0/5 (0%)
MFIA MPV2	0/5 (0%)	0/5 (0%)
MFIA NS1	0/5 (0%)	0/5 (0%)
MFIA MNV	0/5 (0%)	0/5 (0%)
MFIA GDVII	0/5 (0%)	0/5 (0%)
MFIA REO	0/5 (0%)	0/5 (0%)
MFIA EDIM (ROTAA)	0/5 (0%)	0/5 (0%)
MFIA LCMV	0/5 (0%)	0/5 (0%)
MFIA ECTRO	0/5 (0%)	0/5 (0%)
MFIA MAV 1 & 2	0/5 (0%)	0/5 (0%)
MFIA MCMV	0/5 (0%)	0/5 (0%)
MFIA K	0/5 (0%)	0/5 (0%)
MFIA MTLV	0/5 (0%)	0/5 (0%)
MFIA POLY	0/5 (0%)	0/5 (0%)
MFIA HANT	0/5 (0%)	0/5 (0%)
MFIA MPUL	0/5 (0%)	0/5 (0%)
MFIA ECUN	0/5 (0%)	0/5 (0%)
MFIA CARB	0/5 (0%)	0/5 (0%)
MFIA PHV	0/5 (0%)	0/5 (0%)
MFIA LDV	0/5 (0%)	0/5 (0%)
MFIA Anti-Ig Positive Ctrl	5/5 (100%)	5/5 (100%)

Supplemental 4

Infectious Disease PCR	Lab	Wild
LCMV	-	0/10 (0%)
MAV 1 & 2	-	0/10 (0%)
MHV	0/5 (0%)	0/20 (0%)
MNV	-	0/10 (0%)
Mousepox (Ectromelia)	-	0/10 (0%)
Mouse Parvovirus (MPV/MVM) P	0/5 (0%)	0/20 (0%)
MRV (EDIM)	0/5 (0%)	0/20 (0%)
PVM	0/5 (0%)	0/20 (0%)
REO	-	0/10 (0%)
SEND	0/5 (0%)	0/20 (0%)
TMEV/GDVII	0/5 (0%)	0/20 (0%)
Beta Strep Grp A	0/5 (0%)	0/20 (0%)
Beta Strep Grp B	0/5 (0%)	0/20 (0%)
Beta Strep Grp C	0/5 (0%)	0/20 (0%)
Beta Strep Grp G	0/5 (0%)	0/20 (0%)
B. bronchiseptica	0/5 (0%)	0/20 (0%)
B. hinzii	-	0/10 (0%)
Campylobacter Genus	-	0/10 (0%)
C. bovis	-	0/10 (0%)
CAR Bacillus	-	0/10 (0%)
C. kutscheri	0/5 (0%)	0/20 (0%)
C. piliforme	0/5 (0%)	0/20 (0%)
C. rodentium	0/5 (0%)	0/20 (0%)
K. oxytoca	0/5 (0%)	4/20 (20%)
K. pneumoniae	0/5 (0%)	0/20 (0%)
Helicobacter genus	-	0/10 (0%)
M. pulmonis	0/5 (0%)	0/20 (0%)
P. pneumotropicaHeyl	0/5 (0%)	0/20 (0%)
P. pneumotropicaJawetz	0/5 (0%)	0/20 (0%)
Ps. aeruginosa	0/5 (0%)	0/20 (0%)
Salmonella Genus	0/5 (0%)	0/20 (0%)
S. aureus	1/5 (20%)	19/20 (95%)
S. moniliformis	0/5 (0%)	0/20 (0%)
S. pneumoniae	-	0/10 (0%)
Cryptosporidium	-	0/10 (0%)
Demodex	-	0/10 (0%)
Entamoeba	1/5 (20%)	3/20 (15%)
Giardia	0/5 (0%)	0/20 (0%)
Mite	0/5 (0%)	0/20 (0%)
Pinworm	0/5 (0%)	0/20 (0%)
Pneumocystis	0/5 (0%)	0/20 (0%)
P. mirabilis	-	4/10 (40%)
Spironucleus muris	0/5 (0%)	0/20 (0%)
Tritrichomonas genus	-	0/10 (0%)

Supplemental 5

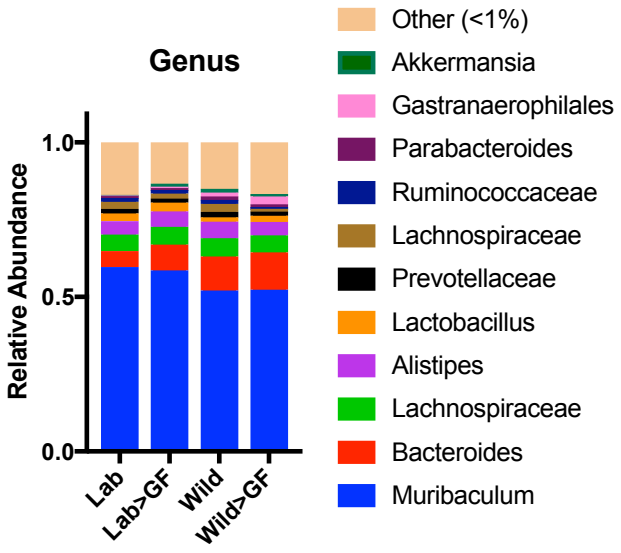

Supplemental 6

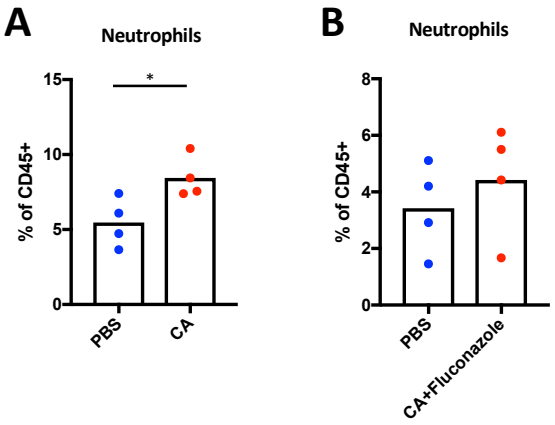

Materials and Methods

C57BL/6J mice were purchased from Jackson Laboratory and bred onsite in an MNV/Helicobacter-free specific pathogen free (SPF) facility at NYU School of Medicine to generate littermates that were randomly assigned to either remain in the institutional vivarium (lab mice) or released into the outdoor enclosures (rewilded mice) to control for the microbiota at the onset of the experiment. As described in the companion paper in which we investigate gene-environment interactions (Lin *et al*), these wild-type (WT) mice were released alongside previously described (*1, 2*) *Nod2*$^{-/-}$, *Atg16l1*$^{T300A/+}$, *Atg16l1*$^{T300A/T300A}$ mice on the C57BL/6J background that were also bred onsite. Outdoor enclosures were previously described (*3, 4*) and the protocols for releasing the laboratory mice into the outdoor enclosure facility were approved by Princeton IACUC.

The enclosures consist of replicate outdoor pens, each measuring about 180 m^2 and fenced by 1.5-m high, zinced iron walls that are buried >80 cm deep and topped with electrical fencing to keep out terrestrial predators. Aluminum pie plates are strung up to deter aerial predators. A (180 × 140 × 70 cm) straw-filled shed is provided in each enclosure, along with two watering stations and a feeding station, so that the same mouse chow used in the laboratory (PicoLab Rodent Diet 20) was provided ad libitum to all mice. Mice outdoors, however, also had access to food sources found within the enclosures, including berries, seeds, and insects. 26-30 mice of mixed genotypes but the same sex were housed in each enclosure for 6-7 weeks. Longworth traps baited with chow were used to catch mice approximately 2 weeks and 4 weeks after release and again 6-7 weeks after release; for each trapping session, two baited traps were set per mouse per enclosure in the early evening, and all traps were checked within 12 hours. For subsequent microbiome assessment, a fresh stool sample was collected directly from the caught mice, flash frozen on dry ice, and stored at −80℃ until

further analysis. Mice were weighed with a spring balance.

116 laboratory mice were released into the outdoor enclosure, and 80 matched littermates were maintained in the institutional vivarium for comparison. For rewilded mice, traps were set regularly until the remaining mice were caught. 104 rewilded mice were caught in the final trapping for terminal analyses. All lab control mice were recovered. Euthanasia was performed by CO2 asphyxiation, and blood, MLNs, and intestinal tissue were harvested. Two rewilded mice failed quality control and were not included in downstream analyses.

Pathogen screen

Randomly selected mice were screened for the presence of infectious agents using EZ-Spot Assessment Plus Multiplexed Fluorometric Immunoassay (MFIA) and PCR Infectious Agent Testing (PRIA) Surveillance Plus Panel (Charles River Laboratories). Dried blood, feces, and body swabs were collected according to submission guidelines.

Flow cytometry analysis. At harvesting, MLNs were removed and the single-cell suspensions were prepared in FACS buffer (HBSS containing 1% BSA, 1mM EDTA, 20mM HEPES, and 1mM sodium pyruvate). The whole blood were also collected in a heparin containing tube and after centrifuging at 2000 rpm for 5 minutes, the designated plasma from supernatant was removed and stored at −80℃ until all samples were collected and analyzed together. After two rounds of red blood cell lysis with 1x RBC lysis buffer (SANTA CRUZ, sc-296258) for 5 minutes and wash with FACS buffer, the single-cell suspensions of whole blood cells were ready for the following staining procedure. MLN and whole blood cells were stained for live/dead with blue reactive dye (catalog#L23105, Invitrogen) and cell surface markers were

labeled with the following antibody panels: Lymphoid panel: CD49b Pacific Blue, CD11b Pacific Blue, CD11c Pacific Blue, CXCR3 Brilliant Violet 421, CD27 Brilliant Violet 510, KLRG1 Brilliant Violet 605, CD3 Brilliant Violet 786, CD127 Brilliant Violet 711, PD1 PerCP/Cy5.5, CD4 APC/Cy7, CD19 PE/Dazzle594, CD8 Brilliant Violet 650, CD43 Alexa Fluor 488, CD62L APC, CD44 PE, CD69 Alexa Fluor 700, (Catalog#108918, #101224, #117322, #126529, #124229, #138419, #100355, #135035, #109120, #100414, #115554, #100742, #121210, #104412, #103008, #14539, Biolegend), CD45 Buv395 (Catalog#564279, BD BioScience), CD25 PE/Cy7 (Catalog#25-0251-86, eBioscience). Myeloid panel: B220 Pacific Blue, CD86 Brilliant Violet 510, CD3 Brilliant Violet 605,CD69 Brilliant Violet 786, CD40 Alexa Fluor 488, Ly6G PerCP/Cy5.5, PDL2 APC, IA/IE APC/Cy7, PDL1 PE, CD64 PE/Dazzle594, F4/80 Alexa Fluor 700, CD11c Brilliant Violet 650 (Catalog#103227, #105040, #100237, #104543, #102910, #127616, #107210, #107628, #124307, #139319, #123130, #117339, Biolegend), Siglec-F Brilliant Violet 421, CD103 Brilliant Violet 711, Ly6C PE/Cy7, CD11b Buv395 (Catalog#562681, #564320, #560593, #563553, BD BioScience). FACS analyses were performed in a ZE5 cell analyzer (BIO-RAD) and recorded FACS data were analyzed by Flowjo v10.4.2.

Histology and imaging

Immunohistochemistry was performed on 10% neutral buffered formalin fixed, paraffin-embedded small intestine and colon tissue. Sections were collected at 5-microns onto plus slides (Fisher Scientific, Cat # 22-042-924) and stored at room temperature prior to use. Unconjugated, rabbit anti-mouse CD 8a, T-cell surface glycoprotein alpha chain, clone D4W2Z (Cell Signaling Cat# 98941 Lot# 1 RRID: unassigned) raised against synthetic peptide corresponding to residues surrounding Asp42 of mouse CD8α protein (5) was used for immunohistochemistry.

Chromogenic Immunohistochemistry was performed on a Ventana Medical Systems Discovery XT instrument with online deparaffinization and using Ventana's reagents and detection kits unless otherwise noted. Samples for CD8a labeling were antigen retrieved in Ventana Cell Conditioner 1 (Tris-Borate-EDTA pH 8.5) at 95° C for 36 minutes. Endogenous peroxidase activity was blocked with 3% hydrogen peroxide for 4 minutes. Antibody was diluted 1:100 in Signal Stain diluent (Cell Signaling Cat# 8112) and incubated for 10 hours at room temperature. CD8a was detected with goat anti-rabbit HRP conjugated multimer. The immune complexes were visualized with 3,3 diaminobenzidene and enhanced with copper sulfate. Slides were washed in distilled water, counterstained with hematoxylin, dehydrated and mounted with permanent media. Appropriate positive and negative controls were run in parallel to study sections.

MLN cell stimulation and cytokine profiling

Single cell suspension of MLN cells were reconstituted in RPMI at 2×10^6 cells/mL, and 0.1 mL was cultured in 96-well microtiter plates that contained 10^7 cfu/mL UV-killed microbes, 10^5 αCD3/CD28 beads, or PBS control. Overnight microbial cultures were reconstituted at 10^8 cfu/mL prior to irradiation. The stimulated microbes are as following: *Staphylococcus aureus* (*6*), *Pseudomonas aeruginosa* (PAO1) (kindly provided by Dr. Andrew Darwin, NYU) (*7*), *Bacillus subtilis* (ATCC 6633), *Clostridium perfringens* (NCTC 10240), *Bacteroides vulgatus* (ATCC 8482), and *Candida albicans* (UC820, kindly provided by Dr. Stefan Feske, NYU). Supernatants were collected after 2 days and stored at −80°C. Concentrations of IL-1α, IL-1β, IL-4, IL-5, IL-6, IL-10, IL-13, IL-17A, CCL2, CCL3, CCL4, CXCL1, IFN-γ, and TNF-α in supernatants were measured using a custom mouse LEGENDplex assay (Biolegend) according to the manufacturer's instructions. Plasma concentrations of IL-1α, IL-1β,

IL-6, IL-10, RANTES, CCL2, CCL3, CCL4, CCL20, CXCL1, CXCL10, TNFα, GM-CSF were measured using a second custom mouse LEGENDplex assay (Biolegend).

16S library preparation and sequencing.

DNA was isolated from stool samples using the NucleoSpin Soil Kit (Macherey-Nagel). Bacterial 16S rRNA gene was amplified at the V4 region using primer pairs and paired-end amplicon sequencing was performed on the Illumina MiSeq system as previously described (*8*). Sequencing reads were processed using the DADA2 pipeline in the QIIME2 software package. Taxonomic assignment was performed against the Silva v132 database. Differential abundance taxa was identified using discrete false-discovery rate (DS-FDR) methodology in different biological groups at a threshold DS-FDR score of 30 (*9*).

Fungal quantification

Fungal DNA was isolated from individual fecal pellets using the NucleoSpin Soil kit (Macherey-Nagel) as described in 16S library preparation. Quantitative PCR was performed using SybrGreen (Roche) on a Roche480II Lightcycler using the following primers: Fungal ITS1-2, Fwd 5'-CTTGGTCATTTAGAGGAAGTAA-3' and Rev 5'-GCTGCGTTCTTCATCGATGC-3'. Relative abundance of fungal-specific internal transcribed spacer (ITS) rDNA was calculated using the ΔC_T method and the values were converted as fold change from the average C_T of control lab mice samples.

Isolation of Wild fungi

Feces or ileocecal contents from re-wilded mice were resuspended in PBS and plated on Sabouraud Dextrose Agar (SDA) with chloramphenicol (25 μg/ml, Sigma) at 25°C for 3 days. Individual colonies were re-grown on SDA plates to acquire the pure strains. Fungal DNA then was extracted from each isolated strains and sequenced using the ITS primers described below to identify the fungal species.

Fungal inoculation

A wild fungi consortium consisting of *A. candidus*, 4 strains of *A. proliferans*, *C. globosum* and *D. Indicus* (corresponding to the fungi on plates (i)–(vii) from Figure 4E was cultured on SDA for 5 days and further cultured in Sabouraud Dextrose broth at 25°C for 2 days. Fungi were passed through a 19-gauge syringe needle several times to break down the mycelium prior to oral gavage into mice and mixed at equal ratios. Mice were orally gavaged with 150 μl of wild fungi consortium every other day for 2 weeks.

ITS library preparation and sequencing

The fungal ITS2 region was targeted for amplification and sequencing with primers that append barcodes and Illumina adapters, similar to those described by Taylor, et al. (*10*). The full primer sequences used were (with XXXXXX indicating barcode sequences, and bold lettering for the ITS2 targeting primers):

AATGATACGGCGACCACCGAGATCTACACXXXXXXXXACACTCTTTCCCT

ACACGACGCTCTTCCGATCTAAAGCCTCCGCTTATTGATATGCTTAART,

CAAGCAGAAGACGGCATACGAGATXXXXXXXXGTGACTGGAGTTCAGAC GTGTGCTCTTCCGATCTGGAACTTTYRRCAAYGGATCWCT. Notably, this results in the Illumina read-one from the reverse (LSU) side of the ITS reference sequence and the read-two from the 5.8S side. The ITS2 region was amplified and Illumina adapters appended by PCR in 25 ul volume with Q5 High-Fidelity 2X master mix (NEB, # M0492L). PCR conditions were as follows: initial denaturation at 95 C for 2 minutes, followed by 32 cycles of 98 C for 15 seconds, 52 C for 20 seconds, 72 C for 45 seconds, and a final 2 minute extension at 72 C. We performed triplicate PCR reactions for each sample, then combined triplicates and cleaned the PCR products with Axygen AxyPrep Mag PCR cleanup beads (Corning, #MAG-PCR-CL-50) using 1.8X volumes of beads diluted to 62.5% in water (v/v) to remove large primer-dimers. Cleaned products were quantified then multiplexed at even abundances and sequenced on an Illumina MiSeq in paired-end mode with 300 cycles each and a 5% PhiX library spike-in to provide increased base diversity. All sequences have been deposited at NCBI under the BioProject PRJNA559026.

ITS sequences analysis. Raw sequences were imported into QIIME2 and read-pairs were joined with the vsearch plugin requiring a minimum length of 300 nucleotides (a completely overlapping pair of reads). Joined reads were then quality filtered and exported to reverse-complement reads with the fastx toolkit (http://hannonlab.cshl.edu/fastx_toolkit/) due to the orientation of our ITS2 primers. Joined, quality-filtered and reverse-complemented reads were re-imported into QIIME2 to employ the ITSxpress plugin in order to trim primers and extract the ITS2 sub-region (*11, 12*). ITS2 sub-region extracted sequences were then denoised with deblur and a trim-length of 150 against the UNITE fungal database reference sequences (version 7) (*13, 14*). Finally, the UNITE database was used to train a naïve

Bayes classifier and to assign fungal taxonomies in QIIME2 (*15*). The community matrix was subsampled at a depth of 906 sequences per sample and Bray-Curtis distances and alpha diversity metrics (observed otus) were calculated within QIIME2.

MLN cell RNA preparation and sequencing

Frozen samples of single cell suspensions from MLN of lab or rewilded mice were thaw to isolate RNA from approximately 10^6 cells by RNeasy Plus Mini Kit (QIAGEN #74136) according to manufacturer's instructions. CEL-seq2 were performed to do RNA sequencing on samples with good RNA qualities (RNA integrity number $\geqq$ 5)

Statistical analysis. An unpaired two-tailed t test was used to evaluate differences between two groups.

Methods References

1. Y. Matsuzawa-Ishimoto *et al.*, *J Exp Med* 214, 3687 (Dec 4, 2017).
2. D. Ramanan, M. S. Tang, R. Bowcutt, P. Loke, K. Cadwell, *Immunity* 41, 311 (Aug 21, 2014).
3. S. A. Budischak *et al.*, *Front Immunol* 8, 1914 (2018).
4. J. M. Leung *et al.*, *PLoS Biol* 16, e2004108 (Mar, 2018).
5. L. Russell *et al.*, *Nat Commun* 9, 5006 (Nov 27, 2018).
6. K. Maurer *et al.*, *Cell Host Microbe* 17, 429 (Apr 8, 2015).
7. D. Srivastava *et al.*, *MBio* 9, (Jul 17, 2018).
8. J. A. Neil *et al.*, *Nat Microbiol*, (Jun 10, 2019).
9. L. Jiang *et al.*, *mSystems* 2, (Nov-Dec, 2017).
10. D. L. Taylor *et al.*, *Appl Environ Microbiol* 82, 7217 (Dec 15, 2016).
11. J. Bengtsson-Palme *et al.*, *Methods in Ecology and Evolution* 4, 914.
12. A. R. Rivers, K. C. Weber, T. G. Gardner, S. Liu, S. D. Armstrong, *F1000Res* 7, 1418 (2018).
13. A. Amir *et al.*, *mSystems* 2, (Mar-Apr, 2017).
14. R. H. Nilsson *et al.*, *Nucleic Acids Res* 47, D259 (Jan 8, 2018).
15. N. A. Bokulich *et al.*, *Microbiome* 6, 90 (May 17, 2018).